Journal of Computer-Aided Molecular Design, **14:** 467–475, 2000.
KLUWER/ESCOM

Pseudoreceptor model for ryanodine derivatives at calcium release channels

Klaus-Jürgen Schleifer
Heinrich-Heine-Universität Düsseldorf, Institute for Pharmaceutical Chemistry, Universitätsstrasse 1, D-40225 Düsseldorf, Germany (E-mail: kjs@pharm.uni-duesseldorf.de)

Received 15 July 1999; Accepted 7 January 2000

Key words: calcium channel, excitation-contraction coupling, Monte Carlo protocol, pseudoreceptor modelling, 3D-QSAR, triad junction

Summary

This paper describes the generation of a pseudoreceptor model for ryanodine receptor (RyR) modulating ryanoids in rabbit skeletal muscle. For this purpose, the molecular modelling software PrGen was applied to correlate experimentally determined and calculated free energies of binding for a set of 15 ryanodine derivatives. The final model indicates a narrow cleft with hydrogen bond donor and acceptor capacities (represented by an Asn) as most crucial for binding the pyrrole carboxylate substituent at C3 of ryanodine. In addition, hydrophobic residues flank the aromatic pyrrole ring (Tyr, Phe, and Ile). Two of those residues (Tyr and Ile) interact with the 2-isopropyl moiety, which seems to contribute to binding. Opposite to the pyrrole locus, a second hydrophobic region (represented by a Leu) restricts ryanodine derivatives in their longitudinal axis and leads to the discrimination of equatorial and axial positioned methyl groups and of polar substituents at C9. Finally, a charged glutamate residue generates strong hydrogen bonding and electrostatic interactions with the hydroxyl groups at C10 and C15. For this binding-site model – composed of six amino acid residues – a correlation for the training set ligands of $R = 0.99$ ($Q^2 = 0.975$) and a root mean square (rms) deviation of 0.568 kcal/mol for the prediction of the binding energies of four test set ligands was obtained. Based on this pseudoreceptor model the putative topology of the real binding site of ryanoids will be discussed.

Introduction

Calcium release through an ion channel present in the terminal cisternae of the sarcoplasmic reticulum initiates contraction in skeletal muscle [1]. This channel is closely connected to transverse tubule membranes to form a structure known as the triad junction. In addition, interactions between this so-called Ca^{2+} release channel and the loop that links domains II and III (II–III loop) of the dihydropyridine-sensitive skeletal muscle L-type Ca^{2+} channel are critical for excitation-contraction coupling in skeletal muscle [1–3]. A better understanding of these essential physiological processes was obtained by the identification, purification, and biochemical characterization of the involved Ca^{2+} release channels from skeletal, cardiac, and neuronal tissue by use of radiolabeled ryanodine as a probe [4–6]. For that reason the Ca^{2+} release channels were designated as ryanodine receptors (RyR1, RyR2, and RyR3, respectively). Besides the most active plant alkaloid ryanodine also Ca^{2+}, ATP, KCl, Mg^{2+}, ruthenium red, caffeine, and calmodulin are modulators of RyR channels [7]. The effects of ryanodine, however, are unique. At submicromolar concentrations, it has been reported to increase channel activity with openings to a full conductance state, and to exhibit partially conducting or subconductance states [1]. At micromolar or higher concentrations, ryanodine produces a closed state of the channel [1]. Due to the lack of any high-resolution 3D-structure of RyRs, there is no direct information about specific receptor/ryanodine interactions to explain the concentration-dependent effects of ryanodine. To date, the only possibility to identify important structural requirements for the

binding process arises from indirect approaches like quantitative structure/affinity relationship (QSAR) investigations of ryanodine derivatives.

Attempting to gain insight into the specific interactions involved in ligand/receptor binding and to yield first information about the putative binding site topology, this paper presents an atomistic pseudoreceptor model derived from correlation of experimentally determined and calculated binding energies of 15 ryanodine derivatives.

Methods

Ligand construction

All investigated ryanodine derivatives were generated in accordance with published ^{1}H-NMR [8] and X-ray data [9] applying the molecular modelling software package SYBYL [10]. In order to yield energetically favourable conformations molecular dynamics simulations (MDS) were carried out in vacuo employing the TRIPOS force field. For this purpose, a simulated annealing protocol was repeated 10 times, starting with a temperature of 1000 K for a period of 1000 fs. Subsequently the temperature was cooled down linearly for 1000 fs to 0 K and the 'frozen' derivative was geometry optimized with the conjugate gradient algorithm. This generated 10 energetically favourable conformers for each ryanoid derivative. A final selection was carried out on the assumption that all considered ryanoids interact with the RyR in a common binding mode. Therefore, the energetically most favourable conformer of the most active derivative (ryanodine, **1**) was used as a template to choose those ryanoid conformers with the highest similarity.

Due to the occurrence of two potential pyridine arrangements of compound **8** (*E*- or *Z*-conformation of the pyridine nitrogen atom relative to the carbonyl oxygen) two further MDS were performed using the *E*-conformer (*E*-**8**) and the *Z*-conformer (*Z*-**8**), respectively, as input structures. For this approach, the simulated annealing protocol described above was repeated 50 times and the simulation periods were increased up to 2000 fs. Subsequently, the lowest energy conformers of *E*-**8** and *Z*-**8** derived from MDS were energy optimized applying the conjugate gradients algorithm until a maximum convergence criterion of 0.05 kcal/(mol · Å) was reached. Furthermore, both minimized conformers were geometry optimized with the semiempiric AM1 method [11] and the potential energies were determined.

ESP partial charges of the minimized structures were derived from the wave functions of single point energy calculations using the AM1 algorithm [11] offered by the SPARTAN software [12].

Pseudoreceptor modelling

Applying the pseudoreceptor modelling software PrGen [13], an atomistic pseudoreceptor model of the RyR binding site was constructed. This programme generates vectors for each functional group of the ligands indicating potential hydrogen bond, lone-pair, or hydrophobic interactions. At the tips of these vectors, individually chosen residue templates of an internal database are automatically docked and oriented. Subsequently, a receptor minimization is carried out by energy minimization of all residues keeping position, orientation, and conformation of the training set ligands unaltered. To achieve a high correlation between experimentally derived and calculated binding energies (ΔG_{exp} vs. ΔG_{cal}) 'correlation coupling' was employed. This additional quantity in the energy term couples the actual root mean square deviation of ΔG_{cal} and ΔG_{exp} to the force field energy of the system. By a straightforward minimization of this term in the course of the correlation-coupled receptor minimization an almost perfect correlation can be enforced. In the next step, the pharmacophore is allowed to relax by minimizing the ligands without constraints while the receptor remains fixed (ligand relaxation). This allows removing strain possibly imposed on the ligands by the receptor during correlation-coupled refinement but usually leads to a less highly correlated model. Therefore, correlation-coupled receptor minimization followed by unconstrained ligand relaxation is repeated until a highly correlated pseudoreceptor model is obtained in the relaxed state (designated as ligand equilibration). To validate the equilibrated receptor, its potency to predict free energies of binding (ΔG_{pred}) for an external set of ligands (test set) is examined. For this purpose, the test set ligands are relaxed within the fixed equilibrated pseudoreceptor, applying the same refinement protocol as described for the training set ligands (see ligand relaxation). The linear regression obtained for the training set is used to estimate free energies of binding for the test set derivatives (for more detailed information see Zbinden [14] and Vedani [15]).

In the present study, coupling constants of 1.0 (receptor equilibration) and 0.3 (ligand equilibration) and a maximal allowed rms of 0.197 kcal/mol for the pre-

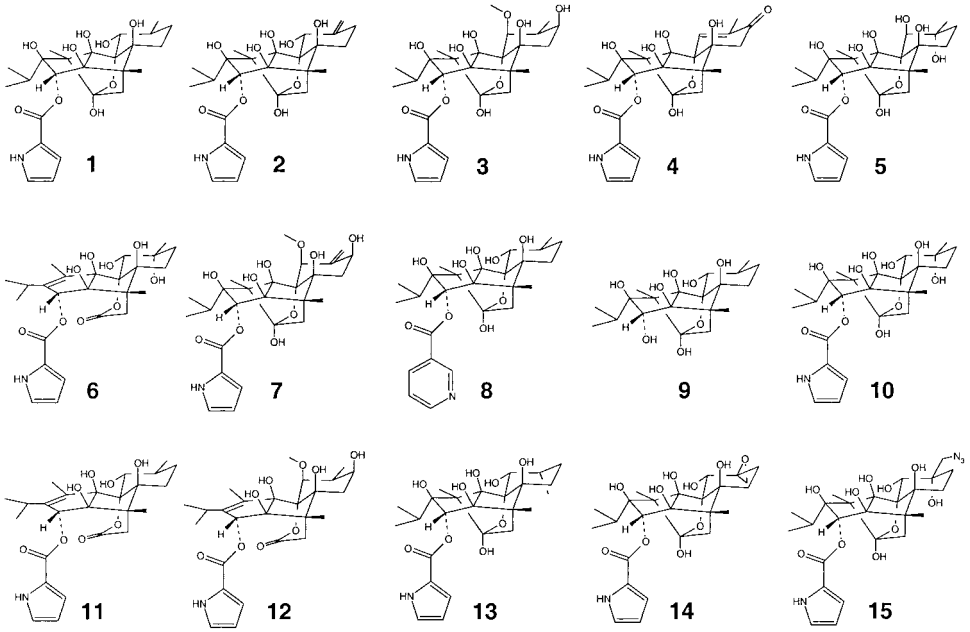

Figure 1. Structural formulae of all ryanodine derivatives used for the pseudoreceptor modelling approach.

dicted versus experimental dissociation constants of all correlation-coupled minimization procedures were used. The target rms deviation was limited to a maximum of 0.236 kcal/mol. Both the training set and the test set structures were relaxed inside the receptor cavity without constraints applying 10 trails of a Monte Carlo procedure. Solvation energies of the ligands were calculated according to Still [16] and entropy corrections were considered following Searle [17]. The essential biological binding data were taken from the literature [18].

Hardware

All computations were carried out on SGI Indigo^2 R10000, SGI O2 R5000 and SGI Indy R4600 workstations.

Results and discussion

Pharmacophore construction

For the generation of a pseudoreceptor model for RyR modulating derivatives in rabbit skeletal muscle, a data set of 15 natural and semi-synthetically varied ryanoids from *Ryania speciosa* Vahl was used [18, 19] (Figure 1).

In order to determine the potential bioactive conformation of all investigated ryanoids, molecular dynamics simulations followed by molecular mechanics geometry optimizations were accomplished. This demonstrated the rigidity of the polycyclic diterpene skeleton, yielded information about the rotational flexibility of the hydroxyl groups, and indicated two potential arrangements of the pyrrole and the pyridine (**8**) ring. Semiempirical AM1 calculations [11] revealed the syn-conformation of the pyrrole (**1** syn vs. anti Δ -0.35 kcal/mol) and the anti-conformation of the pyridine cycle (**8** anti vs. syn Δ -2.26 kcal/mol) as energetically preferred. Moreover, the putative bioactive syn-conformation of the pyrrolocarboxylate is substantiated by X-ray data [9] and further experimental results [20]. Based on these findings, all minimized ryanodine congeners were superimposed on the most active derivative **1** to obtain a common sterical pharmacophore model for the pseudoreceptor modelling approach (Figure 2).

In order to identify crucial structural elements of ryanoid derivatives that contribute to high-affinity binding, the findings provided by structure/affinity (and structure/activity) relationship investigations were considered [18, 21–25], since only a clear determination of important molecular functions yields information about the features and optimal positions of amino acid residues for the model generation.

Figure 2. Stereo plot showing the sterical pharmacophore model of all investigated ryanoid derivatives. For clarity, only the heteroatom-linked hydrogens are displayed (oxygen and nitrogen atoms are darkened).

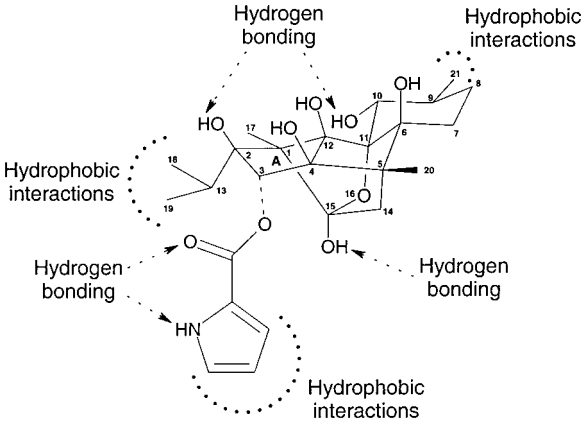

Figure 3. Structural formula of ryanodine (**1**); potential binding site interactions derived from structure/affinity relationship investigations are indicated.

General ryanoid characteristics

The pentacyclic diterpene skeleton of ryanodine carries four cis-hydroxyls at C2, C4, C6, and C12 which, along with the pyrrolocarboxylate NH and C=O, present a hydrophilic face (numbering see Figure 3). An additional hydroxyl at C10 and the hemiketal at C15 are located on the other, hydrophobic side of the molecule. Especially those chemically reactive hydroxyl functions were frequently used for structural modifications like bridging the 4- and 6-hydroxyls as cyclic borates and boronates or blocking the 10- and 12-hydroxyls as cyclic phosphates, phosphonates and phosphoramidates [23]. Additionally, methylations were carried out at several hydroxyl groups and the pyrrole NH function [23]. Those results which are most relevant concerning critical determinants for binding and RyR modulating activity will be discussed in the following paragraphs (K_D values of the mentioned ryanoids are listed in Table 1).

Table 1. Characteristic data of the investigated ryanoid derivatives **1**–**15**

Compound	K_D[a]	ΔG_{exp}[b]	E_{solv}[c]	Randomized[d]
1*	7	−11.572	−16.168	*
2	7	−11.572	−16.923	**13**
3	110	−9.874	−18.204	**12**
4	240	−9.393	−18.229	**15**
5*	210	−9.476	−16.681	*
6*	2600	−7.925	−19.347	*
7*	51	−10.348	−19.861	*
8	1100	−8.455	−15.740	**4**
9	12000	−6.983	−12.025	**8**
10	110	−9.874	−17.455	**2**
11	2900	−7.858	−16.806	**3**
12	5200	−7.498	−18.920	**11**
13	13	−11.190	−15.904	**9**
14	36	−10.563	−19.478	**14**
15	78	−10.086	−17.394	**10**

*Test set ligands applied for the prediction of ΔG_{exp} values.
[a]Dissociation constants [nM] determined in a [^{3}H]ryanodine binding assay at 37 °C by Welch [18].
[b]Free energies of binding [kcal/mol] derived from the K_D values according to the Gibbs-Helmholtz equation.
[c] Solvation energies in kcal/mol according to Still [16].
[d]Automatically assigned ligand numbers to randomly scramble the ΔG_{exp} values employed for a significance test of the final pseudoreceptor model (e.g., ryanoid **2** was investigated using the ΔG_{exp} value of compound **13**).

3-Pyrrole carboxylate

The importance of the pyrrole locus becomes evident by comparing the binding affinities of ryanodine (**1**), ryanodyl nicotinate (**8**) and ryanodol (**9**). While the carbonyl group as a potential hydrogen bond acceptor is present at compounds **1** and **8**, hydrogen donor capacities are found for the pyrrole NH function of **1** and, although not in the same region, also for the alcoholic hydroxyl group at C3 of derivative **9**. Obviously, both of these functions are necessary to achieve high binding affinity although the H-bond accepting

capacity seems to be more important. However, also the hydrogen bond donor characteristics should contribute to binding, since it was shown that methylation of the pyrrole NH function leads to an 8-fold decrease in affinity [23]. The RyR modulating activity of the N-methylated compound, however, is not altered [23].

2-Isopropyl group

There is no definite proof of the necessity of an isopropyl group at C2 for strong receptor binding, but all investigated pyrrole-containing ryanoids have a common hydrophobic area along the hydrocarbon edge of the pyrrole and on either side of the isopropyl substituent. Thus, it is tempting to assume this moiety as a preferred hydrophobic counterpart of the binding site.

2-Hydroxyl group

In vertebrate tissue a 3- (canine ventricle) to 8-fold (rabbit muscle) decrease in binding affinity was observed for 2-deoxy-2(13)-dehydroryanodine differing only by the dehydrated 2-hydroxyl group from ryanodine [23]. Since the strongest effect of this variation was observed in rabbit muscle cells, which have also been used to determine the binding affinities of the presented ryanoid derivatives, this hydroxyl group might be involved in binding.

15-Hydroxyl group

Unfortunately, there are no experimental data available for ryanoid derivatives with chemical variations only at this particular position (e.g., 15-methoxy group), although in acidic medium ryanodine (**1**) dehydrates easily and gives the anhydroryanodine derivative **11**. However, not only the hydroxyl group at C15 but also at C2 are separated. In addition, induced by the $\Delta^{1,2}$ double bond important modifications in the ryanoid skeleton (i.e. the geometry of ring A) and the orientation of the isopropyl group are affected. The dimethylated derivative N,15-O-dimethylryanodine was tested in a receptor assay and had been found to be 28-fold less potent compared with ryanodine [21]. An unambiguous interpretation of this finding is not possible since besides the desired modification at C15 also the pyrrole NH as postulated H-bond donor is altered. Nevertheless, one possible explanation for the weak binding affinities of anhydroryanodine derivatives (**6**, **11**, and **12**) compared to derivatives with a hydroxyl group at C15 could be a missing hydrogen bond donor interaction with the binding site.

10-Hydroxyl group

With the exception of compounds **3**, **4**, **7** and **12** all of the investigated ryanoid derivatives carry an equatorial hydroxyl function at C10. Oxidation to the 10-oxo ryanodine derivative reduces the binding affinity to 30%, and 10-benzoyloxy-ryanodine retains only about 4% of the binding potency determined for ryanodine [24]. Simultaneous methylation of the 4- and 10-hydroxyl groups reduces affinity to RyR in rabbit muscle to 3.5%, whereas the 4-methoxylated ryanodine derivative (unaltered 10-position) retains 30% of the original affinity, revealing the importance of the 10-hydroxy function [23]. Furthermore, theoretically accomplished comparative molecular field analyses (CoMFA) indicated the substituent at the 10-position of ryanoids as exerting the greatest influence on fractional conductance of RyR [23].

9-Substituents

Only minor effects are detected by changing the substitution pattern at C9. However, the comparison of ryanodine (**1**) with dehydroryanodine (**2**) and 9-epiryanodine (**13**) makes obvious that a methyl group in equatorial (**1**) or pseudoequatorial (**2**) orientation is more favourable compared with an axial position (**13**). On the other hand, by comparing the ryanoid derivatives **10** and **15** it is indicated that steric bulk in an equatorial arrangement has almost no influence on the binding affinity. Insertion of a second substituent at position 9 is accompanied with a loss of affinity (**13** vs. **14**). A stronger effect is induced by the introduction of an additional axially positioned hydroxyl group (**1** vs. **10**) indicating this position as unfavourable for polar groups. However, the same variation shows no effects for anhydroryanoid derivatives (compare **6** vs. **11**) giving rise to the suspicion of a modified binding orientation of these derivatives.

Pseudoreceptor generation

A training set of 11 ryanoid derivatives (see Table 1) was chosen for the generation of a reasonable pseudoreceptor model employing the software package PrGen [13]. In order to select appropriate residues for pseudoreceptor construction, information derived from the above-discussed structure/affinity relationships was considered (Figure 3).

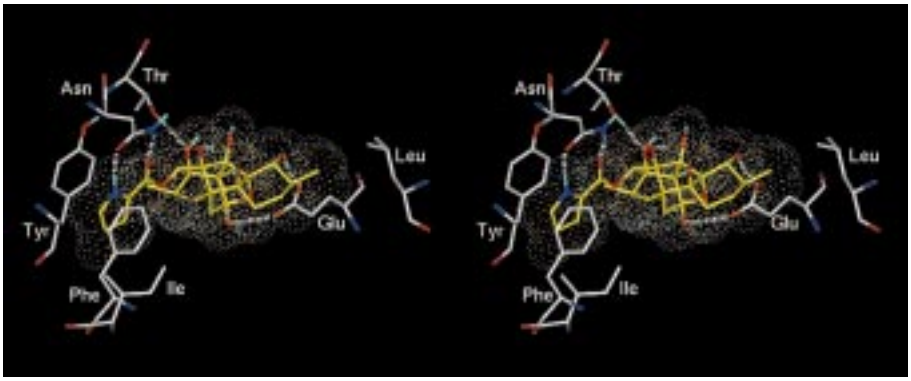

Figure 4. Stereo plot of pseudoreceptor model 1 composed of seven amino acid residues. Only ryanodine (yellow coloured carbons) as a representative of the test set ligands is displayed with its van der Waals surface to clarify the binding mode. Hydrogen bonds are indicated as dotted lines (colour code: carbon grey, oxygen red, nitrogen blue, hydrogen cyan).

On this basis, one amino acid residue acting simultaneously as H-bond acceptor and donor (e.g., asparagine or tyrosine) was placed complementary to the pyrrole NH and the carbonyl oxygen functions. In addition, two hydrophobic residues (e.g., tyrosine or methionine) were arranged parallel and a further isoleucine below the pyrrole ring to obtain a tight binding pocket for this primary determinant of high-affinity ryanodine binding. At the same time, two of those hydrophobic residues and the C_β-methyl group of a threonine, which was applied to form a hydrogen bond with the 2-hydroxyl group, were allowed to interact with the 2-isopropyl moiety. To evaluate the hypothesis of a critical binding site interaction with the 15-hydroxyl group several H-bond acceptors (e.g., threonine, glutamine, or glutamic acid) were probed. Furthermore, this residue was positioned in such a way that a further interaction with the 10-hydroxyl group was feasible. Finally, a hydrophobic residue (e.g., isoleucine) was selected to enable discrimination between the different substitution patterns at C9.

Although a model composed of 7 amino acid residues might not be sufficient to represent the topology of the true biological binding site, no further residues were chosen for pseudoreceptor generation. Furthermore, also 'virtual particles', provided by the software PrGen to represent bulk properties, have not been considered, since the aim of this study was to elucidate only crucial requirements of the ryanodine binding site. Use of further amino acid residues or virtual particles, however, would enhance the number of variables and descriptors, and thereby – caused by the sum of all these interactions – lead to overemphasized models. Significance of the essential contacts of the surrogate, however, would be decreased.

In order to achieve optimum positions of the manually placed residues, a receptor equilibration was performed allowing translation, rotation, and torsional variations only for receptor residues, whereas the ligands were kept fixed in their original arrangement. Subsequently, the pharmacophore was allowed to relax within the binding pocket. Repeating these two steps several times, the so-called ligand equilibration yielded a pseudoreceptor model (Figure 4) with a coefficient $R = 0.988$ for the correlation of experimentally detected (ΔG_{exp}) and calculated free energies of binding (ΔG_{cal}). In the next step, the remaining four test set ligands were introduced into the fixed pseudoreceptor model and relaxed yielding a root mean square (rms) deviation for the predicted binding energies of 0.447 kcal/mol (Table 2).

In this model (designated as model 1) the pyrrole carboxylate is shielded by four amino acid residues (Asn, Phe, Tyr, and Ile). A threonine (Thr) generates a hydrogen bond to the 2-hydroxyl group and the previously mentioned Phe and Ile interact with the isopropyl substituent at C2. A glutamate (Glu) acts as counterpart of the 15- and 10-hydroxyl functions by forming two H-bonds and a leucine (Leu) serves as hydrophobic residue complementary to C21 (Figure 4).

In order to examine the importance of some individual pseudoreceptor residues to contribute to binding, first the threonine was deleted. At the same time, the isoleucine, positioned below the pyrrole ring, was shifted in direction to C19. Restarting the receptor and ligand equilibration procedures, model 2 was obtained with $R = 0.991$ for the training set ligands. For the following prediction of the test set ligands an almost optimal rms = 0.283 kcal/mol was found, implicat-

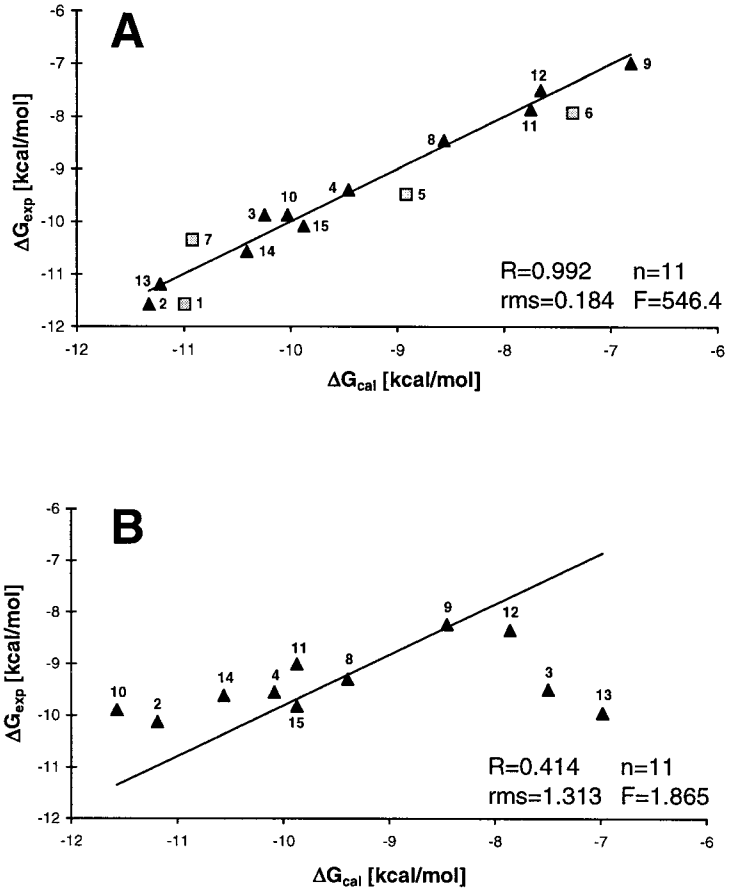

Figure 5. The graphs illustrate: (A) the result derived from pseudoreceptor model 2 (Monte-Carlo) for the correlation of experimentally determined (ΔG_{exp}) and via pseudoreceptor calculated/predicted (ΔG_{cal}) free energies of binding for the training set (triangles) and the test set ligands (squares); (B) the result obtained for the re-generated pseudoreceptor model 2 applying randomly scrambled binding data for the training set ligands (triangles).

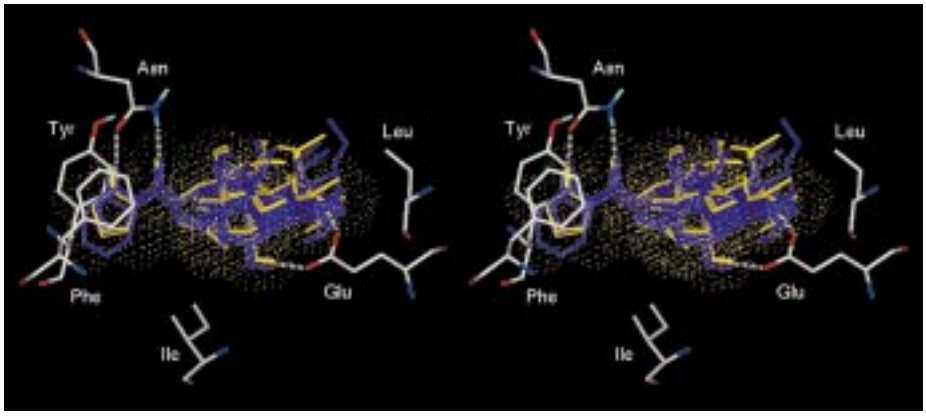

Figure 6. Stereo view of pseudoreceptor model 2 MC composed of six amino acid residues. The training set (purple coloured) and the test set ligands (yellow coloured) are displayed. The yellow dots represent the van der Waals surface of ryanodine (**1**) and the dotted lines indicate hydrogen bonding interactions (the H-bond from Glu to the 10-hydroxyl functions is partially covered by the ligands).

Table 2. Statistical analysis of the presented pseudoreceptor models

Statistics	Model 1	Model 2	Model 3
R	0.988	0.991	0.988
rms	0.219	0.190	0.219
Q^2	0.964	0.976	0.968
rms*	0.447	0.283	0.879
R (MC)	0.991	0.992	n.d.
rms (MC)	0.189	0.184	n.d.
Q^2 (MC)	0.975	0.975	n.d.
rms* (MC)	0.661	0.568	n.d.
rms* (MC)[a]	0.229	0.257	n.d.
R (rand.)	0.451	0.414	n.d.
rms (rand.)	1.288	1.314	n.d.
Q^2 (rand.)	−0.099	−0.163	n.d.

R, correlation coefficient yielded by the correlation of experimentally detected and calculated/predicted free energies of binding; rms, root mean square; Q^2, prediction derived from a leave-one-out cross-validation.
*, results obtained for the test set ligands.
MC, a Monte Carlo protocol was applied.
[a]The original training set in its pharmacophoric arrangement was used as test set.
rand., automatically randomized experimental binding data used to prove the significance of the final pseudoreceptor models (see Table 1).
n.d., not determined.

ing the insignificance of the 2-hydroxyl function as a potential binding site stabilizing contact.

Analysis of model 2 revealed only minor effects of the leucine opposite to C21, which generates even repulsive contacts to some ligands. Therefore, this leucine was deleted and the complete receptor generation was repeated. The resulting model 3 (R = 0.988) with a prediction for the test set compounds of rms = 0.879 kcal/mol demonstrates the necessity of such hydrophobic contacts for pseudoreceptor models with high accuracy (Table 2).

Subsequently, a Monte Carlo (MC) protocol was employed for ligand equilibration and test set minimization, allowing a more exhaustive exploration of the pseudoreceptor cavity with respect to ligand positions, orientations, and conformations associated with the lowest potential energy. This yielded deviations for the prediction of the test set ligands of rms = 0.661 kcal/mol (model 1 MC) and rms = 0.568 kcal/mol (model 2 MC, Figure 5).

The adequateness of the optimization procedure used for the test set ligands was tested by re-inserting the training set in its original pharmacophoric orientation into the final receptor models 1 MC and 2 MC and subjecting it to the same minimization protocol as has been used for the test set. Analysis of the results derived from this optimization indicated an almost perfect prediction for the training set ligands (Table 2).

In a final step, the statistical significance of the correlation between experimentally detected and via pseudoreceptor models calculated binding energies was evaluated. Therefore, the same training set ligands in their original pharmacophoric geometries were inserted into the initial models (i.e. prior to receptor equilibration). However, not the correct experimental binding constants but randomly scrambled data were used (Table 1). The following pseudoreceptor generation, performed by receptor and ligand equilibration yielded no reliable model (R = 0.414) for the automatically assigned ΔG_{exp} values (Figure 5 and Table 2).

The final pseudoreceptor model is composed of six amino acid residues (Figure 6). The key functions are taken by an asparagine (Asn) acting simultaneously as hydrogen bond donor and acceptor for the pyrrole carboxylate, and a glutamate stabilizing the 10- and 15-hydroxyl groups via hydrogen bonding and electrostatic interactions. In addition to the Asn, two aromatic residues (Phe and Tyr) as well as an isoleucine wrap the pyrrole locus. The 2-isopropyl substituent generates favourable van der Waals contacts with Phe and Ile. A leucine opposite to the pyrrole cleft completes the necessary requirements of this pseudoreceptor model.

Based on this hypothetical model, the real ryanodine binding site could be characterized as follows. Most critical for the binding of ryanodine derivatives is a hydrophobic cleft allowing hydrogen bond interactions to the pyrrole carboxylate functions of the ligands. Opposite to this hot spot, a second hydrophobic region produces favourable interactions with equatorial and pseudoequatorial oriented methyl groups, whereas polar substituents especially in an axial position are unfavourable. A hydrophilic, possibly water filled region between these enclosing lipophilic poles would substantiate the presence of a charged (glutamate) residue in the pseudoreceptor models. If ryanodine is fixed at the binding site, both hydrophobic regions are perfectly occupied. In addition, the anionic residue saturates two hydroxyl functions of the ligand (probably C10 and C15) whereby the loss of solvation energy for the ligand and the charged amino acid residue could be compensated. Fixed in this position, the hydrophilic edge of the ryanoids is accessible to

water and therefore all cis-hydroxyl functions could be solvated. This proposed binding mode would provide optimal direct ligand/binding site interactions without the usual decrease of solvation energy.

Acknowledgements

I am grateful to Prof. Dr. H.-D. Höltje, Heinrich-Heine-Universität Düsseldorf, for his continual support, for helpful discussions and for providing all hardware and software facilities, and thanks are due to E. Tot for technical assistance.

Supplementary material available

The 3D-coordinates of all discussed ligands and models are available electronically upon request (kjs@pharm.uni-duesseldorf.de).

References

1. Sutko, J.L., Airey, J.A., Welch, W. and Ruest, L., Pharmacol. Rev., 49 (1997) 53.
2. Leong, P. and MacLennan, D.H., J. Biol. Chem., 273 (1998) 7791.
3. Saiki, Y., El-Hayek, R. and Ikemoto, N., J. Biol. Chem., 274 (1999) 7825.
4. Pessah, I.N., Waterhouse, A.L. and Casida, J.E., Biochem. Biophys. Res. Commun., 128 (1985) 449.
5. Takeshima, H., Nishimura, S., Matsumoto, T., Ishida, H., Kangawa, K., Minamino, N., Matsuo, H., Ueda, M., Hanaoka, M., Hirose, T. and Numa, S., Nature, 339 (1989) 439.
6. Zorzato, F., Fujii, J., Otsu, K., Phillips, M., Green, N.M., Lai, F.A., Meissner, G. and MacLennan, D.H., J. Biol. Chem., 265 (1990) 2244.
7. Sutko, J.L. and Airey, J.A., Physiol. Rev., 76 (1996) 1027.
8. Jefferies, P.R., Lam, W.-W., Toia, R.F. and Casida, J.E., J. Agric. Food Chem., 40 (1992) 509.
9. Ruest, L. and Dodier, M., Can. J. Chem., 74 (1996) 2424.
10. SYBYL v. 6.5, Tripos Associates, Inc., St. Louis, MO, USA.
11. Dewar, M.J.S., Zoebisch, E.G., Healy, E.F. and Stewart, J.J.P., J. Am. Chem. Soc., 107 (1985) 3902.
12. SPARTAN 4.1.1, Wavefunction, Irvine, CA, USA.
13. PrGen 1.5.6, Zbinden, P., Biographics Laboratory, Basel, Switzerland, 1997.
14. Zbinden, P., Dobler, M., Folkers, G. and Vedani, A., Quant. Struct-Act. Relat., 17 (1998) 122.
15. Vedani, A., Zbinden, P., Snyder, J.P. and Greenidge, P.A., J. Am. Chem. Soc., 117 (1995) 4987.
16. Still, W.C., Tempczyk, A., Hawley, R.C. and Hendrickson, T., J. Am. Chem. Soc., 112 (1990) 6127.
17. Searle, M.S. and Williams, D.H., J. Am. Chem. Soc., 114 (1992) 10690.
18. Welch, W., Ahmad, S., Airey, J.A., Gerzon, K., Humerickhouse, R.A., Besch, H.R. Jr, Ruest, L., Deslongchamps, P. and Sutko, J.L., Biochemistry, 33 (1994) 6074.
19. Ruest, L., Taylor, D.R. and Deslongchamps, P., Can. J. Chem., 63 (1985) 2840.
20. Kaye, P.T., Macrae, R., Meakins, D.D. and Patterson, C.H., J. Chem. Soc. Perkin II, (1980) 1631.
21. Waterhouse, A.L., Pessah, I.N., Francini, A.O. and Casida, J.E., J. Med. Chem., 30 (1987) 710.
22. Welch, W., Sutko, J.L., Mitchell, K.E., Airey, J. and Ruest, L., Biochemistry, 35 (1996) 7165.
23. Jefferies, P.R., Blumenkopf, T.A., Gengo, P.J., Cole, L.C. and Casida, J.E., J. Med. Chem., 39 (1996) 2331.
24. Jefferies, P.R., Gengo, P.J., Watson, M.J. and Casida, J.E., J. Med. Chem., 39 (1996) 2339.
25. Welch, W., Williams, A.J., Tinker, A., Mitchell, K.E., Deslongchamps, P., Lamothe, J., Gerzon, K., Bidasee, K.R., Besch, H.R. Jr, Airey, J.A., Sutko, J.L. and Ruest, L., Biochemistry, 36 (1997) 2939.